Integrated all-optical pulse regenerator in chalcogenide waveguides

Vahid G. Ta'eed, Mehrdad Shokooh-Saremi, Libin Fu, David J. Moss, Martin Rochette, Ian C. M. Littler, and Benjamin J. Eggleton

Centre for Ultrahigh-bandwidth Devices for Optical Systems (CUDOS), School of Physics, University of Sydney, New South Wales 2006, Australia

Yinlan Ruan and Barry Luther-Davies

Centre for Ultrahigh-bandwidth Devices for Optical Systems (CUDOS), Laser Physics Centre, The Australian National University, Canberra, ACT 0200, Australia

Received June 10, 2005; revised manuscript received July 11, 2005; accepted July 15, 2005

We report a fully integrated, passive, all-optical regenerator capable of terabit per second operation, based on a highly nonlinear chalcogenide (As_2S_3) glass rib waveguide followed by an integrated Bragg grating bandpass filter. We demonstrate a clear nonlinear power transfer curve with 1.4 ps optical pulses, capable of improving the signal-to-noise ratio and reducing the bit error rate for digital signals. © 2005 Optical Society of America

OCIS codes: 050.2770, 070.4340, 130.3120, 230.1150.

Optical data transmission speeds have recently reached the stage where laboratory demonstrations at 640 Gbits/s have been reported.[1,2] At these bit rates any signal processing must be done all optically since electronic processing speeds are currently limited to 40 Gbits/s. To date, however, the only reported devices capable of operating at these speeds have been based in optical fiber[3–7]—all-optical photonic integrated circuits capable of operating at >1 Tbit/s have yet to be demonstrated.

To demonstrate all-optical photonic integrated circuits, a suitable, highly nonlinear optical material is required. Chalcogenide glass has attracted significant attention[8–12] in recent years as a promising nonlinear optical material in the 1550 nm wavelength range, owing to its large n_2 (up to 1000× silica) and low two-photon absorption (good figure of merit), the ability to tailor material properties via stoichiometry, as well as its photosensitivity, allowing the fabrication of photowritten gratings and waveguides. In addition, since the nonlinearity in chalcogenide glass is dominated by the pure virtual material nonlinearity ($\chi^{(3)}$ in the form of n_2) with an intrinsic response time of $\leqslant$100 fs, it is potentially much faster than devices based on real carrier dynamics such as semiconductor optical amplifiers.

In this paper we present a fully integrated all-optical signal regenerator capable of terabit per second rates based on chalcogenide glass. It operates on a principle proposed by Mamyshev,[3] producing a nonlinear power transfer curve through a combination of spectral broadening via self-phase modulation (SPM) in a straight nonlinear waveguide segment followed by linear spectral filtering by an integrated waveguide Bragg grating filter. We demonstrate a clear nonlinear power transfer curve suitable for all-optical signal regeneration (reshaping), with 1.4 ps pulses at peak power levels from a few watts up to 55 W.

Figure 1 illustrates the principle of operation of the device reported here. A straight nonlinear rib waveguide is followed by a waveguide Bragg grating filter, with the grating passband offset from the signal wavelength by more than the signal optical bandwidth so that at low intensities the optical signal is blocked by the filter. At higher intensities (representing logical "1") the pulses undergo SPM induced spectral broadening so that a portion of the spectrum overlaps with the transmission band pass filter and consequently is transmitted. At still higher intensities the signal experiences significant broadening, and the power within the transmission band pass saturates. The resulting S-shaped nonlinear power transfer curve [Fig. 1(c)] is a hallmark of optical regenerators (for reshaping) and has the effect of reducing noise on both the "0" and "1" signals, improving both the optical signal-to-noise ratio and, for bits that contain information, the bit error rate[13] (BER).

The device reported here is the result of recent advances in low-loss rib waveguides[12] and high-quality Bragg gratings in chalcogenide glass (As_2S_3). The chalcogenide waveguides were fabricated by pulsed laser deposition of a 2.4 μm thick As_2S_3 film, with a refractive index of 2.38, followed by photolithography and reactive-ion etching to form a 5 cm long, 4 μm wide rib waveguide with a rib height of 1.1 μm, and then overcoated with a polymer film transparent in the visible. The fiber–waveguide–fiber insertion loss (with high-NA fiber, 4 μm mode field diameter) was 9.3 dB, of which ~1.5 dB was propagation loss, equating to a coupling efficiency of ~3.9 dB per facet (including about 0.8 dB of Fresnel reflection loss from the material refractive index mismatch). The intrinsic material loss of the chalcogenide thin film[12] is <0.1 dB/cm, so the majority of the loss arises from waveguide roughness due to photolithography and dry etching.

Waveguide gratings were written near the exit facet of the waveguide by using a Sagnac interferometer along with a cw 532 nm doubled Nd:YAG laser having a coherence length of ~4 mm, which provided compensated refractive index apodization. The

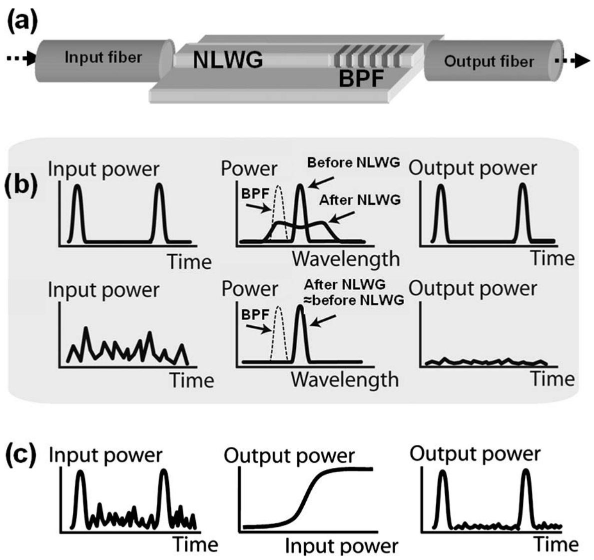

Fig. 1. Principle of device operation. (a) The optical regenerator consists of a 5 cm long nonlinear As_2S_3 rib waveguide (NLWG) where SPM-induced spectral broadening occurs, followed by an integrated Bragg grating bandpass filter (BPF), offset from the signal frequency, near the exit facet. (b) Input noise experiences less SPM spectral broadening than the signal does, and hence is attenuated more than the signal after filtering. (c) This produces a nonlinear power transfer curve and results in both optical signal-to-noise ratio and BER improvement

sample was exposed with 10 mW for 60 s, resulting in gratings with an estimated index change $\Delta n = 0.004-0.005$. The extremely high quality of the gratings in terms of both grating spectral width (>6 nm each at 3 dB), and in-band rejection (depth, >25 dB at the grating center), as well as very low out-of-band sidelobes, was critical for the successful performance of this device.

We demonstrated the device performance with 1.4 ps, full width at half-maximum pulses from a mode-locked figure 8 laser,[14] with the light passed through a polarization controller and then a custom optical amplifier (designed to minimize excess spectral broadening), resulting in 8.75 MHz repetition rate pulses at peak powers up to 1.2 kW, nearly transform limited with a spectral width of 1.9 nm, tunable from 1530 to 1560 nm. The output of the amplifier was butt coupled into the waveguide by using a short (to minimize spectral broadening within the fiber) 20 cm length of standard single-mode telecommunications fiber followed by 5 mm of high-NA fiber spliced on the end to improve coupling efficiency to the waveguide. The output of the waveguide was then directed either into a powermeter, an optical spectrum analyzer, or an optical autocorrelator.

Figure 2(a) shows the pulse spectra for 1.8 ps pulses after they have passed through a bare waveguide with no grating present, showing significant broadening with increasing input peak power, due to SPM equivalent to a nonlinear optical phase shift (ϕ_{NL}) of approximately $3\pi/2$, which was spectrally symmetric. The maximum peak power in the waveguide was 53 W, corresponding to a maximum intensity of ~1.0 GW/cm^2. Our experimental results are consistent with calculations that assume an n_2 in As_2S_3 of about 100× silica, similar to other reports in the literature.[12] We did not observe any nonlinear effects due to two-photon absorption at the power levels in our experiments, and estimate a minimum value for a figure of merit of >10, again consistent with previous measurements.[12] We verified that SPM-induced spectral broadening by the amplifier was negligible and that no photodarkening occurred.

Figure 2(b) shows the transmission spectrum of the waveguide Bragg grating for TE polarization. The grating in fact consisted of two gratings offset from each other to produce an overall rejection bandwidth of 16.3 nm with a 2.8 nm wide passband in the middle. The TM polarized grating was separated by ~8 nm from the TE grating due to waveguide birefringence, and so these experiments were carried out with TE polarized light. We could launch TE polarized pulses to better than a 20 dB extinction ratio by adjusting the polarization controller before the amplifier. The pulse center wavelength was tuned to within the rejection band of the Bragg grating on the longer wavelength side of the passband. As seen in Fig. 2(c), this resulted in low transmission at low input power, since the filter rejection bandwidth was much wider than the 3 dB spectral bandwidth of the input pulse. As the input pulse power was increased, SPM broadened the spectrum so that power was transmitted through the passband of the grating. Figure 3 shows the resulting power transfer curve, obtained by adjusting the relative signal-to-filter wavelength offset to optimize the device performance, which exhibits a clear nonlinear S shape, required for optical regeneration.

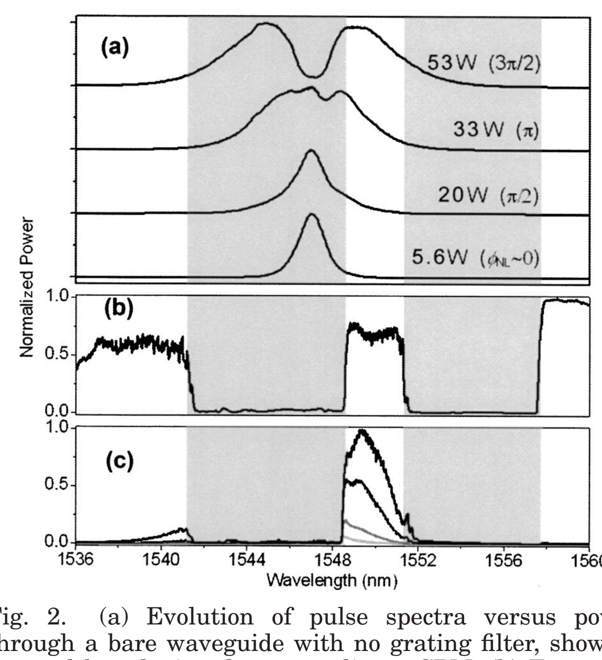

Fig. 2. (a) Evolution of pulse spectra versus power through a bare waveguide with no grating filter, showing spectral broadening due to nonlinear SPM. (b) Transmission spectrum of the bandpass filter (formed by two sequential offset gratings) for TE polarized light, showing a passband of 2.8 nm near 1555.0 nm, offset by 3 nm from the carrier wavelength. (c) Sliced SPM broadened output spectra after the filter.

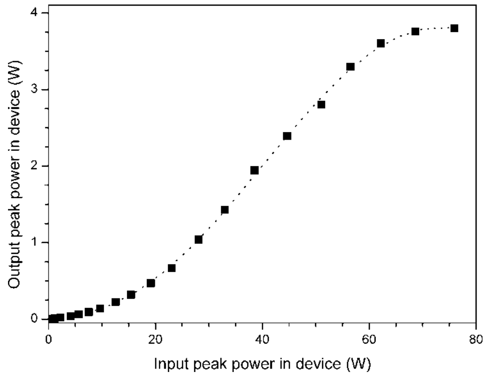

Fig. 3. Resulting S-shaped power transfer curve, enabling suppression of noise and BER improvement. The dotted curve is a guide to the eye.

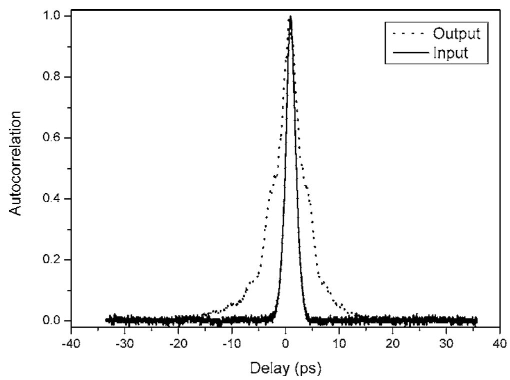

Fig. 4. Autocorrelation of input (solid) and output (dotted) pulses at high power. Pulses broaden from an inferred Gaussian width of 1.4 ps to 3.3 ps, because of grating edge dispersion and pulse–filter mismatch.

The autocorrelation of the input and output pulses at high power is shown in Fig. 4, indicating that the output pulses were broadened slightly to ~3 ps. This broadening is not due to either waveguide dispersion or material dispersion in the passive waveguide section (both of which are negligible on this length scale) but is due mainly to the grating dispersion near the edge of the stop band.[15] Optimizing the grating passband shape and width is expected[15] to reduce this broadening and can provide flexibility, even tunability,[16] for reconfigurable regeneration.

While this device operates at peak powers up to 55 W and was tested with low-duty-cycle optical pulses, practical devices would need to operate at subwatt power levels and with high-duty-cycle (e.g., 33% return to zero) optical pulses. By increasing the device length to 50 cm through the use of serpentine or spiral structures, increasing the material nonlinearity (by using As_2Se_3 rather than As_2S_3, for example) and by decreasing the waveguide area by a factor of 10 (to 1 μm^2), a reduction in operating power by 2 orders of magnitude should be achievable, resulting in subwatt power level operation. Furthermore, the increased (normal) dispersion of longer waveguides would linearize the frequency chirp of the output pulses, reducing pulse distortion and improving transfer function characteristics.[5]

In conclusion, we demonstrate an integrated all-optical signal regenerator consisting of a nonlinear waveguide followed by an integrated Bragg grating filter in chalcogenide glass. It operates through the virtual material nonlinear (Kerr) response in chalcogenide glass and is therefore capable of terabit per second bit rates. We demonstrate a clear nonlinear power transfer curve by using 1.4 ps optical pulses, which would result in optical signal-to-noise ratio reduction and bit error rate improvement in optical links.

This work was produced with the assistance of the Australian Research Council (ARC). CUDOS (the Centre for Ultrahigh-bandwidth Devices for Optical Systems) is an ARC Centre of Excellence. M. Shokooh-Saremi appreciates the support of the Iranian Ministry of Science, Research and Technology as well as Iran Telecommunication Research Centre. V. G. Ta'eed's e-mail address is vahid@physics.usyd.edu.au.

References

1. M. Nakazawa, H. Kubota, K. Suzuki, E. Yamada, and A. Sahara, IEEE J. Sel. Top. Quantum Electron. **6**, 363 (2000).
2. N. Yamada, S. Nogiwa, and H. Ohta, IEEE Photon. Technol. Lett. **16**, 1125 (2004).
3. P. V. Mamyshev, in *24th European Conference on Optical Communication* (IEEE, 1998), p. 475.
4. G. Raybon, Y. Su, J. Leuthold, R.-J. Essiambre, T. Her, C. Joergensen, P. Steinvurzel, and K. D. K. Feder, in *Optical Fiber Communication Conference*, Vol. 69 of OSA Trends in Optics and Photonics Series (Optical Society of America, 2002), p. FD10-1.
5. P. Z. Huang, A. Gray, I. Khrushchev, and I. Bennion, IEEE Photon. Technol. Lett. **16**, 2526 (2004).
6. F. Ohman, S. Bischoff, B. Tromborg, and J. Mork, in *Proceedings of 2003 5th International Conference on Transparent Optical Networks* (IEEE, 2003), Vol. 2, p. 41.
7. O. Leclerc, B. Lavigne, E. Balmefrezol, P. Brindel, L. Pierre, D. Rouvillain, and F. Seguineau, J. Lightwave Technol. **21**, 2779 (2003).
8. M. Asobe, Opt. Fiber Technol. **3**, 142 (1997).
9. K. Tanaka, J. Non-Cryst. Solids **338**, 340 (2004).
10. R. E. Slusher, G. Lenz, J. Hodelin, J. Sanghera, L. Brandon Shaw, and I. D. Aggarwal, J. Opt. Soc. Am. B **21**, 1146 (2004).
11. S. Spälter, H. Y. Hwang, J. Zimmermann, G. Lenz, T. Katsufuji, S.-W. Cheong, and R. E. Slusher, Opt. Lett. **27**, 363 (2002).
12. Y. Ruan, W. Li, R. Jarvis, N. Madsen, A. Rode, and B. Luther-Davies, Opt. Express **12**, 5140 (2004).
13. M. Rochette, J. N. Kutz, J. L. Blows, D. Moss, J. T. Mok, and B. Eggleton, IEEE Photon. Technol. Lett. **17**, 908 (2005).
14. T. O. Tsun, M. K. Islam, and P. L. Chu, Opt. Commun. **141**, 65 (1997).
15. G. Lenz, B. J. Eggleton, C. R. Giles, C. K. Madsen, and R. E. Slusher, IEEE J. Quantum Electron. **34**, 1390 (1998).
16. I. C. M. Littler, M. Rochette, and B. J. Eggleton, Opt. Express **13**, 3397 (2005).